Electronic Supplementary Material (ESI) for RSC Advances.
This journal is © The Royal Society of Chemistry 2016

Electronic Supplementary Information for: α, β-Substitution Effect of Dialkylphosphinic Acids on Lanthanide Extraction

*Ruobing Du, Donghai Yu, Huaying An, Suhui Zhang, Gang Zhao, Ji-Chang Xiao**

Key Laboratory of Organofluorine Chemistry, Shanghai Institute of Organic Chemistry, Chinese Academy of Sciences, 345 Lingling Rd, Shanghai, 200032, China

E-mail: jchxiao@sioc.ac.cn, Tel: +86-21-54925340

Contents

1. Energies and structure parameters

1.1. Table S1. Dimerization energies and structure parameters of extractants

Table S1. The structure parameters for monomers and dimmers of the extractants, and the dimerization energy change. (unit: kJ/mol or Å)

HL	p118	p127	p1c6	p218	p227
ΔG^{D}	-32.35	-36.00	-56.83	-29.39	-53.59
d_{O-H}^{M}	0.9633	0.9636	0.9633	0.9630	0.9633
d_{O-H}^{D}	1.0182	1.0207	1.0182	1.0149	1.0160
$d_{OH\cdots O}^{D}$	1.5454	1.5273	1.5341	1.5485	1.5459

ΔG^{D}, The differences of Gibbs free energies of dimerization reaction.

${d_{O-H}}^{M}$, The O-H bond length of monomer.

${d_{O-H}}^{D}$, The average O-H bond length of dimer.

${d_{OH\cdots O}}^{D}$, The average $OH\cdots O$ hydrogen bond length of dimer.

Strong hydrogen bond was formed between the hydroxyl hydrogen of the dimers and the the oxygen of another phosphoryl group, leading to the elongation of the O-H bond. Only the arithmetic mean values of ${d_{O-H}}^{D}$ and ${d_{OH\cdots O}}^{D}$ were collected due to they are close. The substituent showed almost no influence on ${d_{O-H}}^{M}$, which is agreement with their close pK_a data (Table 1). However, β-substituent demonstrated a greater influence on ΔG^{D} than α-substituent. For example, ΔG^{D}(P127) - ΔG^{D}(P118) = -3.65 kJ/mol, and ΔG^{D}(P227) - ΔG^{D}(P218) = -24.12 kJ/mol. In addition, the larger substituent is useful for dimerization.

1.2. Table S2-S4. Structure parameters of model complexes

Table S2. The average WBIs of Ln-L in simplified extraction complexes of DD model.

HL	p118	p127	p1c6	p218	p227
La^{3+}	0.3865	0.3809	0.3835	0.3919	0.3890
Pr^{3+}	0.4346	0.4143	0.4182	0.4278	0.4240
Nd^{3+}	0.4129	0.4058	0.4097	0.4149	0.4150
Dy^{3+}	0.3970	0.4044	0.3955	0.4083	0.4058
Ho^{3+}	0.4118	0.4097	0.4008	0.4081	0.4096
Yb^{3+}	0.4046	0.4070	0.3985	0.4054	0.4064
Lu^{3+}	0.3813	0.3827	0.3756	0.3828	0.3838

Table S3. The average bond length of Ln-L in simplified extraction complexes of DD model. (Å)

	p118	p127	p1c6	p218	p227
La^{3+}	2.3825	2.3931	2.3935	2.3768	2.3825
Pr^{3+}	2.3301	2.3548	2.3546	2.3371	2.3449
Nd^{3+}	2.3262	2.3190	2.3372	2.3206	2.3280
Dy^{3+}	2.2413	2.2367	2.2517	2.2284	2.2333
Ho^{3+}	2.2176	2.2231	2.2377	2.2222	2.2216
Yb^{3+}	2.1914	2.1892	2.2039	2.1888	2.1880
Lu^{3+}	2.1815	2.1798	2.1946	2.1794	2.1786

Table S4. The bond length of hydroxyl and hydrogen bond in simplified extraction complexes of DD model. (Å)

	p118	p127	p1c6	p218	p227

La^{3+}	$d_{OH\cdots O}^{C}$	1.5351	1.5304	1.5543	1.5540	1.5405
	d_{O-H}^{C}	1.0227	1.0250	1.0177	1.0183	1.0197
Pr^{3+}	$d_{OH\cdots O}^{C}$	1.5434	1.5303	1.5507	1.5524	1.5379
	d_{O-H}^{C}	1.0205	1.0254	1.0184	1.0189	1.0203
Nd^{3+}	$d_{OH\cdots O}^{C}$	1.5347	1.5293	1.5492	1.5528	1.5365
	d_{O-H}^{C}	1.0226	1.0257	1.0187	1.0188	1.0206
Dy^{3+}	$d_{OH\cdots O}^{C}$	1.5206	1.5767	1.5316	1.5142	1.5350
	d_{O-H}^{C}	1.0255	1.0131	1.0211	1.0261	1.0223
Ho^{3+}	$d_{OH\cdots O}^{C}$	1.5311	1.5718	1.5378	1.5430	1.5313
	d_{O-H}^{C}	1.0237	1.0136	1.0200	1.0215	1.0229
Yb^{3+}	$d_{OH\cdots O}^{C}$	1.5004	1.5691	1.5343	1.5326	1.5299
	d_{O-H}^{C}	1.0282	1.0140	1.0207	1.0237	1.0235
Lu^{3+}	$d_{OH\cdots O}^{C}$	1.5040	1.5684	1.5341	1.5332	1.5298
	d_{O-H}^{C}	1.0279	1.0142	1.0208	1.0237	1.0235

$d_{OH\cdots O}^{C}$, The hydrogen bond length of $OH\cdots O$ in DD model complexes.

d_{O-H}^{C}, The bond length of O-H in DD model complexes.

The structure parameters of DD model complexes were collected in Table S2-Table S4. Only the average WBIs and bond length of Ln-L are were collected because they are close. The DD model showed similar WBIs and bond length of Ln-L as DM model. According to the $d_{OH\cdots O}^{C}$ and d_{O-H}^{C}, as listed in Table S4, the coordinated dimer remained almost the same as the non-coordinated one.

2. Comparison of three simplified model and experimental result

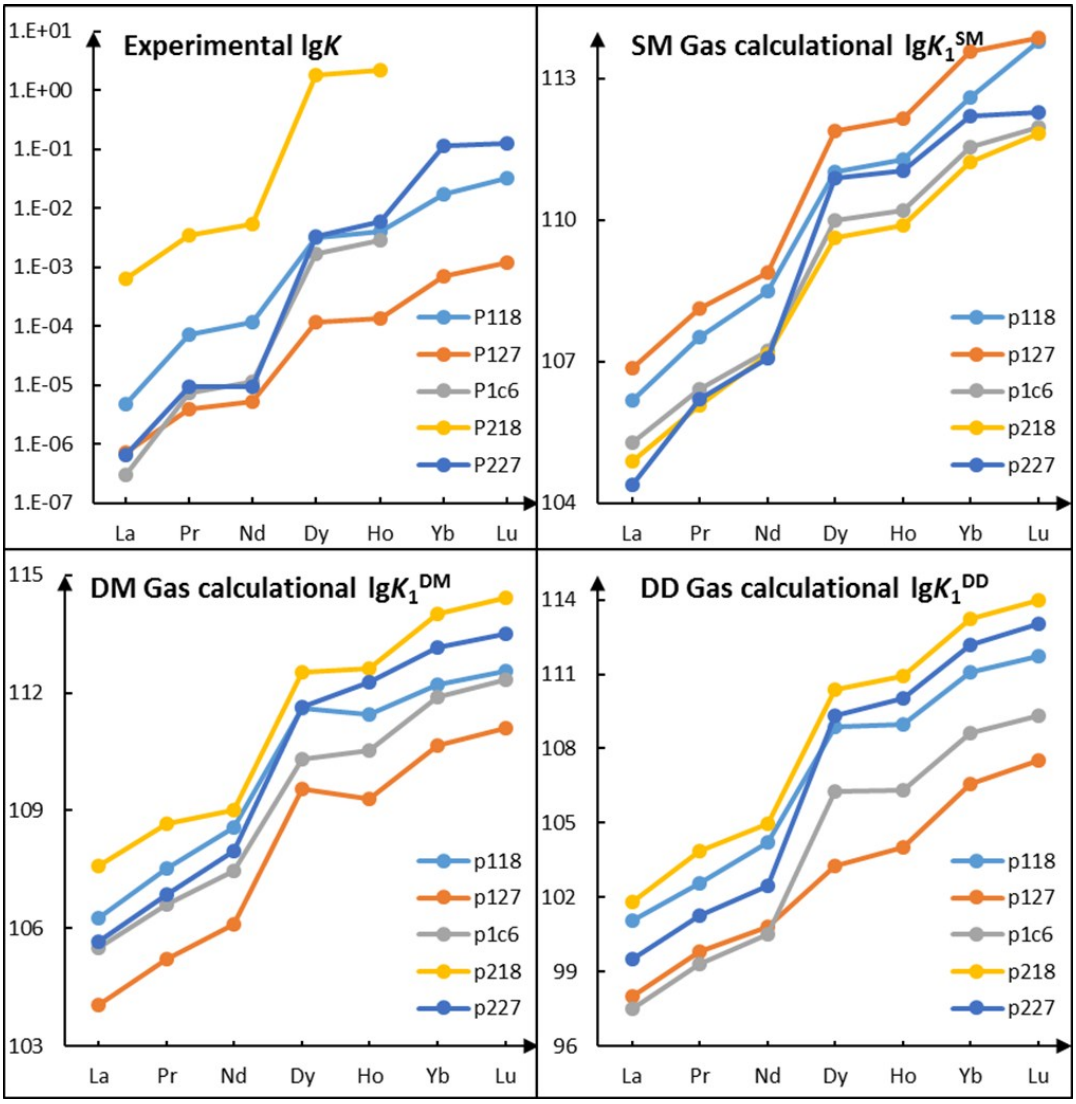

Figure S1. The experimental extraction equilibrium constants, lg*K*; the calculational first stability equilibrium constants, SM (lgK_{1}^{SM}), DM (lgK_{1}^{DM}), and DD (lgK_{1}^{DD}).

A comparison of lg*K*, lgK_{1}^{SM}, lgK_{1}^{DM}, lgK_{1}^{DD} showed that lgK_{1}^{SM} is much different from the others in trend. P127 (orange line) showed the highest extractability for all ions, which is in contradiction with the experimental results. This indicated that the SM model is unreasonable. Consequently, only the DM and DD model complexes are used to investigate the M-L interaction.

3. Geometries of all structures

3.1 Figure S2. Labels of all atoms and hydrated lanthanide ions

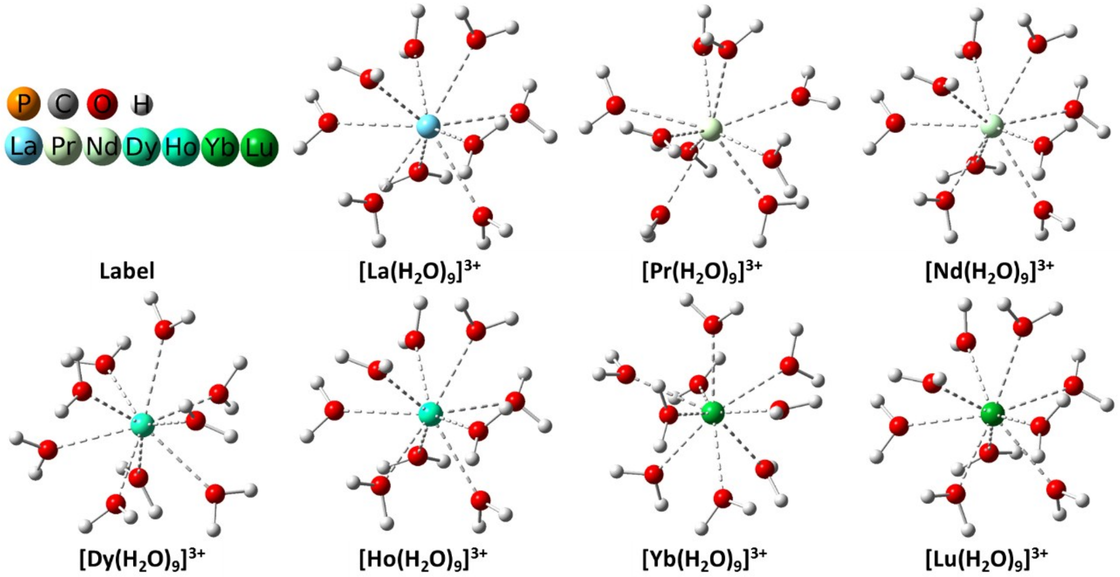

Label **$[La(H_2O)_9]^{3+}$** **$[Pr(H_2O)_9]^{3+}$** **$[Nd(H_2O)_9]^{3+}$**

$[Dy(H_2O)_9]^{3+}$ **$[Ho(H_2O)_9]^{3+}$** **$[Yb(H_2O)_9]^{3+}$** **$[Lu(H_2O)_9]^{3+}$**

Figure S2. The Labels of all atoms, and the hydrated trivalent lanthanide metal ions $\left[Ln(H_2O)_9\right]^{3+}$.

3.2 Figure S3. Monomers and dimers of extractants

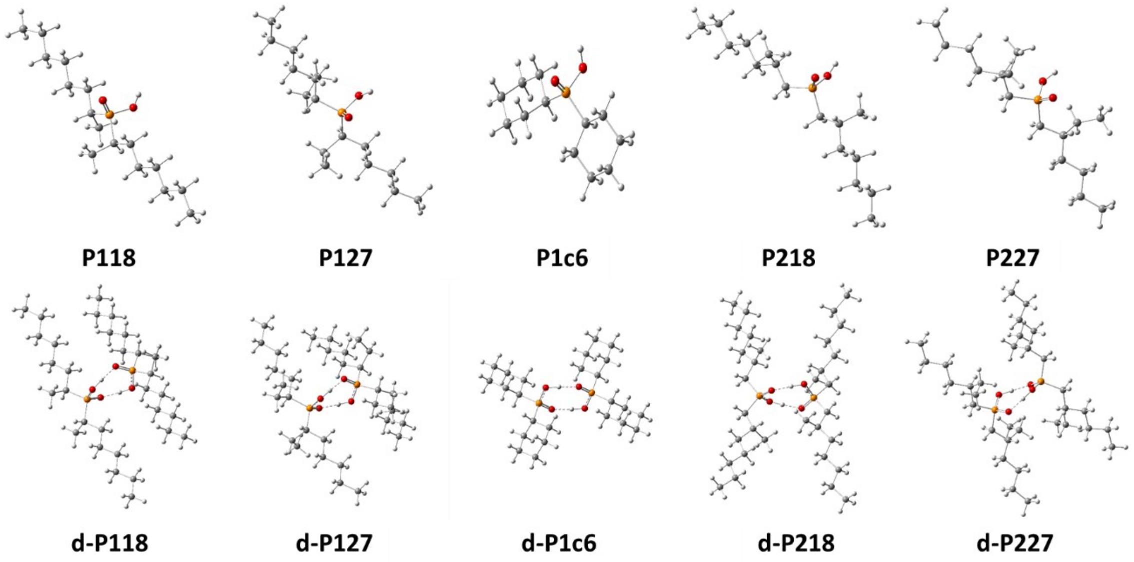

P118 **P127** **P1c6** **P218** **P227**

d-P118 **d-P127** **d-P1c6** **d-P218** **d-P227**

Figure S3. The ball and bond structure of extractant monomer and dimer.

3.3 Figure S4-Figure S6. Simplified model complexes

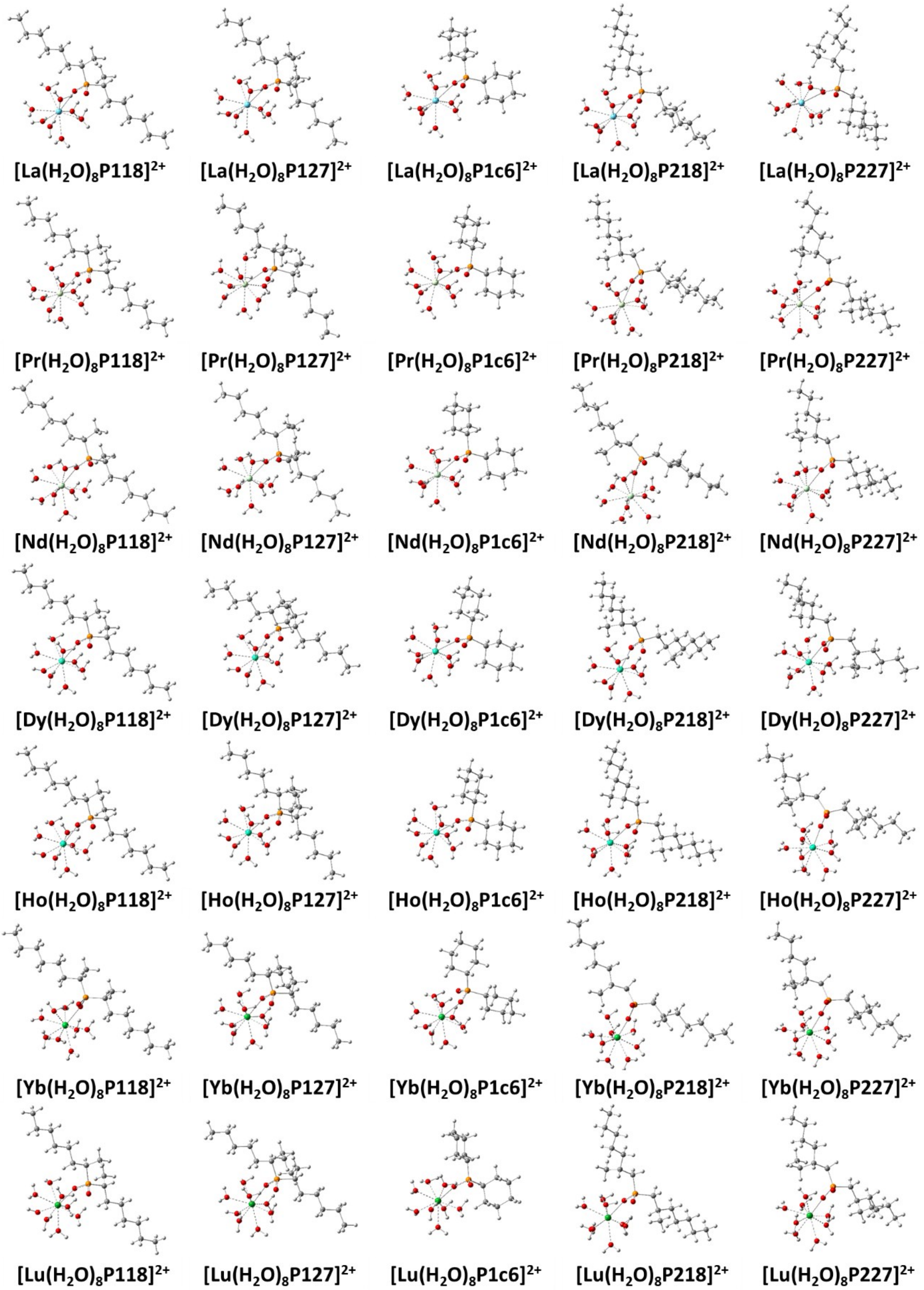

$[La(H_2O)_8P118]^{2+}$ $[La(H_2O)_8P127]^{2+}$ $[La(H_2O)_8P1c6]^{2+}$ $[La(H_2O)_8P218]^{2+}$ $[La(H_2O)_8P227]^{2+}$

$[Pr(H_2O)_8P118]^{2+}$ $[Pr(H_2O)_8P127]^{2+}$ $[Pr(H_2O)_8P1c6]^{2+}$ $[Pr(H_2O)_8P218]^{2+}$ $[Pr(H_2O)_8P227]^{2+}$

$[Nd(H_2O)_8P118]^{2+}$ $[Nd(H_2O)_8P127]^{2+}$ $[Nd(H_2O)_8P1c6]^{2+}$ $[Nd(H_2O)_8P218]^{2+}$ $[Nd(H_2O)_8P227]^{2+}$

$[Dy(H_2O)_8P118]^{2+}$ $[Dy(H_2O)_8P127]^{2+}$ $[Dy(H_2O)_8P1c6]^{2+}$ $[Dy(H_2O)_8P218]^{2+}$ $[Dy(H_2O)_8P227]^{2+}$

$[Ho(H_2O)_8P118]^{2+}$ $[Ho(H_2O)_8P127]^{2+}$ $[Ho(H_2O)_8P1c6]^{2+}$ $[Ho(H_2O)_8P218]^{2+}$ $[Ho(H_2O)_8P227]^{2+}$

$[Yb(H_2O)_8P118]^{2+}$ $[Yb(H_2O)_8P127]^{2+}$ $[Yb(H_2O)_8P1c6]^{2+}$ $[Yb(H_2O)_8P218]^{2+}$ $[Yb(H_2O)_8P227]^{2+}$

$[Lu(H_2O)_8P118]^{2+}$ $[Lu(H_2O)_8P127]^{2+}$ $[Lu(H_2O)_8P1c6]^{2+}$ $[Lu(H_2O)_8P218]^{2+}$ $[Lu(H_2O)_8P227]^{2+}$

Figure S4. The ball and bond structure of SM model complex $[Ln(H_2O)_8L]^{2+}$.

As shown in Figure S4, the α-substituent in SM model complex diverged from the metal ion, which can’t show the interaction between the side chain and the coordinated water molecule, the repulsion between alkyl groups. This is why P127 showed the highest extractability (Figure S1).

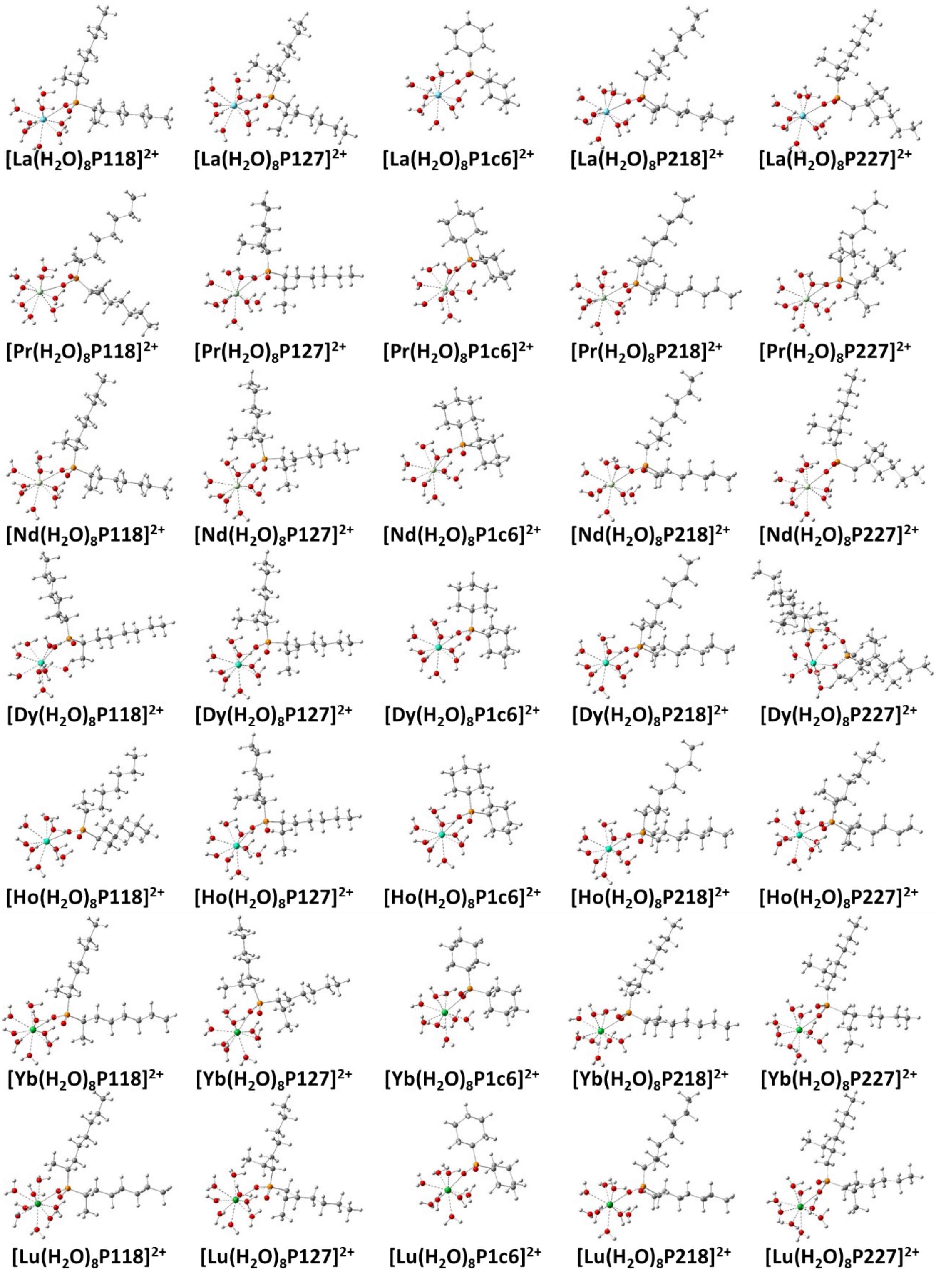

$[La(H_2O)_8P118]^{2+}$ $[La(H_2O)_8P127]^{2+}$ $[La(H_2O)_8P1c6]^{2+}$ $[La(H_2O)_8P218]^{2+}$ $[La(H_2O)_8P227]^{2+}$

$[Pr(H_2O)_8P118]^{2+}$ $[Pr(H_2O)_8P127]^{2+}$ $[Pr(H_2O)_8P1c6]^{2+}$ $[Pr(H_2O)_8P218]^{2+}$ $[Pr(H_2O)_8P227]^{2+}$

$[Nd(H_2O)_8P118]^{2+}$ $[Nd(H_2O)_8P127]^{2+}$ $[Nd(H_2O)_8P1c6]^{2+}$ $[Nd(H_2O)_8P218]^{2+}$ $[Nd(H_2O)_8P227]^{2+}$

$[Dy(H_2O)_8P118]^{2+}$ $[Dy(H_2O)_8P127]^{2+}$ $[Dy(H_2O)_8P1c6]^{2+}$ $[Dy(H_2O)_8P218]^{2+}$ $[Dy(H_2O)_8P227]^{2+}$

$[Ho(H_2O)_8P118]^{2+}$ $[Ho(H_2O)_8P127]^{2+}$ $[Ho(H_2O)_8P1c6]^{2+}$ $[Ho(H_2O)_8P218]^{2+}$ $[Ho(H_2O)_8P227]^{2+}$

$[Yb(H_2O)_8P118]^{2+}$ $[Yb(H_2O)_8P127]^{2+}$ $[Yb(H_2O)_8P1c6]^{2+}$ $[Yb(H_2O)_8P218]^{2+}$ $[Yb(H_2O)_8P227]^{2+}$

$[Lu(H_2O)_8P118]^{2+}$ $[Lu(H_2O)_8P127]^{2+}$ $[Lu(H_2O)_8P1c6]^{2+}$ $[Lu(H_2O)_8P218]^{2+}$ $[Lu(H_2O)_8P227]^{2+}$

Figure S5. The ball and bond structure of DM model complex $[Ln(H_2O)_8L]^{2+}$.

The DM model complexes shown in Figure S5 are obviously different from the SM model complexes shown in Figure S4. The DM model complexes showed the distorted extractant chains, except for P1c6 series. This model was derived from the roughly optimized stoichiometric complex $[Ln(HL_2)_3]$. One extractant monomer unit was retained, with others replaced with water molecules. Consequently, the repulsion between alkyl groups was partly reflected, and lgK_1^{DM} is similar to lgK in Figure S1.

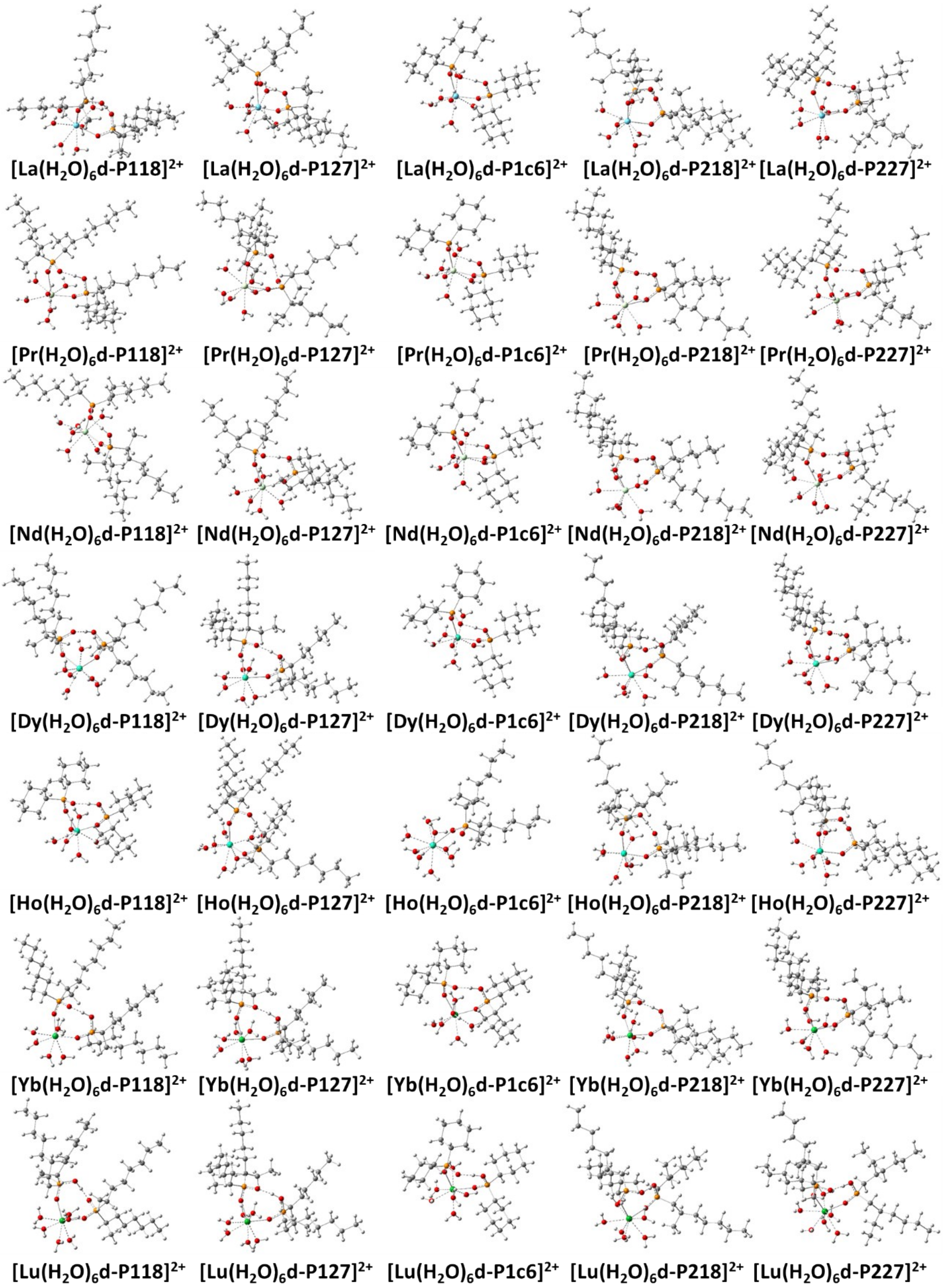

$[La(H_2O)_6d\text{-}P118]^{2+}$ $[La(H_2O)_6d\text{-}P127]^{2+}$ $[La(H_2O)_6d\text{-}P1c6]^{2+}$ $[La(H_2O)_6d\text{-}P218]^{2+}$ $[La(H_2O)_6d\text{-}P227]^{2+}$

$[Pr(H_2O)_6d\text{-}P118]^{2+}$ $[Pr(H_2O)_6d\text{-}P127]^{2+}$ $[Pr(H_2O)_6d\text{-}P1c6]^{2+}$ $[Pr(H_2O)_6d\text{-}P218]^{2+}$ $[Pr(H_2O)_6d\text{-}P227]^{2+}$

$[Nd(H_2O)_6d\text{-}P118]^{2+}$ $[Nd(H_2O)_6d\text{-}P127]^{2+}$ $[Nd(H_2O)_6d\text{-}P1c6]^{2+}$ $[Nd(H_2O)_6d\text{-}P218]^{2+}$ $[Nd(H_2O)_6d\text{-}P227]^{2+}$

$[Dy(H_2O)_6d\text{-}P118]^{2+}$ $[Dy(H_2O)_6d\text{-}P127]^{2+}$ $[Dy(H_2O)_6d\text{-}P1c6]^{2+}$ $[Dy(H_2O)_6d\text{-}P218]^{2+}$ $[Dy(H_2O)_6d\text{-}P227]^{2+}$

$[Ho(H_2O)_6d\text{-}P118]^{2+}$ $[Ho(H_2O)_6d\text{-}P127]^{2+}$ $[Ho(H_2O)_6d\text{-}P1c6]^{2+}$ $[Ho(H_2O)_6d\text{-}P218]^{2+}$ $[Ho(H_2O)_6d\text{-}P227]^{2+}$

$[Yb(H_2O)_6d\text{-}P118]^{2+}$ $[Yb(H_2O)_6d\text{-}P127]^{2+}$ $[Yb(H_2O)_6d\text{-}P1c6]^{2+}$ $[Yb(H_2O)_6d\text{-}P218]^{2+}$ $[Yb(H_2O)_6d\text{-}P227]^{2+}$

$[Lu(H_2O)_6d\text{-}P118]^{2+}$ $[Lu(H_2O)_6d\text{-}P127]^{2+}$ $[Lu(H_2O)_6d\text{-}P1c6]^{2+}$ $[Lu(H_2O)_6d\text{-}P218]^{2+}$ $[Lu(H_2O)_6d\text{-}P227]^{2+}$

Figure S6. The ball and bond structure of DM model complex $\left[Ln(H_2O)_6HL_2\right]^{2+}$.

The DD model was also derived from the roughly optimized stoichiometric complex $\left[Ln(HL_2)_3\right]$. But one extractant dimer unit was retained. For this model, $lgK\,_1^{DD}$ also agreed well with the experimental lgK.

4. Complete Gaussian 09 reference

Complete Gaussian 09 reference (*Ref.* 30)
Gaussian 09, Revision D.01, M. J. Frisch, G. W. Trucks, H. B. Schlegel, G. E. Scuseria, M. A. Robb, J. R. Cheeseman, G. Scalmani, V. Barone, B. Mennucci, G. A. Petersson, H. Nakatsuji, M. Caricato, X. Li, H. P. Hratchian, A. F. Izmaylov, J. Bloino, G. Zheng, J. L. Sonnenberg, M. Hada, M. Ehara, K. Toyota, R. Fukuda, J. Hasegawa, M. Ishida, T. Nakajima, Y. Honda, O. Kitao, H. Nakai, T. Vreven, J. A. Montgomery, Jr., J. E. Peralta, F. Ogliaro, M. Bearpark, J. J. Heyd, E. Brothers, K. N. Kudin, V. N. Staroverov, T. Keith, R. Kobayashi, J. Normand, K. Raghavachari, A. Rendell, J. C. Burant, S. S. Iyengar, J. Tomasi, M. Cossi, N. Rega, J. M. Millam, M. Klene, J. E. Knox, J. B. Cross, V. Bakken, C. Adamo, J. Jaramillo, R. Gomperts, R. E. Stratmann, O. Yazyev, A. J. Austin, R. Cammi, C. Pomelli, J. W. Ochterski, R. L. Martin, K. Morokuma, V. G. Zakrzewski, G. A. Voth, P. Salvador, J. J. Dannenberg, S. Dapprich, A. D. Daniels, O. Farkas, J. B. Foresman, J. V. Ortiz, J. Cioslowski, and D. J. Fox, Gaussian, Inc., Wallingford CT, 2013.

5. Synthesis and Characterization

5.1 Synthesis

The dialkylphosphinic acid used in this study was synthesized via free-radical addition, using sodium hypophosphite monohydrate, alkene, and a peroxide initiator. The procedure was as follows. $NaH_2PO_2 \cdot H_2O$ (20 mmol), acetic acid (20 mmol), alkene (42 mmol), di-t-butyl peroxide (DTBP; 8 mmol), and dimethylformamide (10 mL) were placed in a 50-mL autoclave. The mixture was reacted at 130 °C for 10 h. The solvent was removed under reduced pressure. The residue was dissolved in water, acidified with HCl, and extracted with diethyl ether. The ether layer was washed with water and the solvent was evaporated. The residue pH was adjusted to 7 with 1 M NaOH, and the neutral impurities were removed using diethyl ether. The solvent was removed and the residue was heated in a vacuum at 100 °C. The dialkylphosphinic acid was obtained in 87% yield.

5.2 Characterization

P118

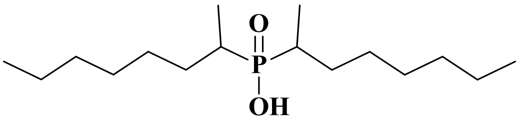

Bis(1-methylheptyl)phosphinic acid: ^1H NMR (400 MHz, CDCl3) δ 11.72 (s, 1H), 1.82-1.69 (m, 4H), 1.49 (d, J = 8Hz, 2H), 1.26 (br, 16 H), 1.15-1.08 (dd, ^1J = 8Hz, ^2J = 12 Hz, 6H), 0.86 (t, J = 12 Hz, 6H).

^{13}C NMR(100 MHz, CDCl3) δ 31.24, 30.08, 29.19, 28.7, 28.20, 28.01, 26.89, 26.77, 22.12, 13.54, 11.45, 11.27. ^{31}P NMR (162 MHz, CDCl3) δ 65.91. ESI-MS(m/z): 291.1 (M+H$^+$). HRMS: calcd for $C_{16}H_{36}O_2P$ 291.2447; found 291.2445.

P127

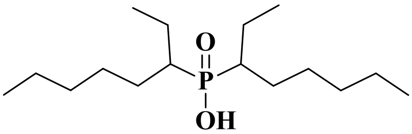

Bis(1-ethylhexyl)phosphinic acid: ^{1}H NMR (400 MHz, CDCl3) δ 11.63 (s, 1H), 1.82-1.43 (m, 12H), 1.34-1.22 (m, 10H), 1.00 (t, J = 12 Hz, 6H), 0.86 (t, J = 12 Hz, 6H). ^{13}C NMR (100 MHz, CDCl3) δ 37.3, 36.48, 31.54, 27.09, 27.00, 26.13, 21.99, 19.66, 13.54, 11.84, 11.75. ^{31}P NMR (162 MHz, CDCl3) δ 66.40. ESI-MS(m/z): 291.1 (M+H$^+$). HRMS: calcd for $C_{16}H_{36}O_2P$ 291.2447; found 291.2445.

P1c6

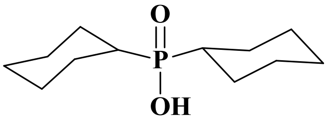

Bis-cyclohexyl phosphinic acid: ^{1}H NMR (400 MHz, CDCl3) δ 11.76 (s, 1H), 1.86-1.78 (m, 8H), 1.71-1.63 (m, 4H), 1.43-1.37 (m, 4H), 1.21 (t, J = 12 Hz, 6H). ^{31}P NMR (162 MHz, CDCl3) δ 61.2. ESI-MS(m/z): 291.1 (M+H$^+$).

P218

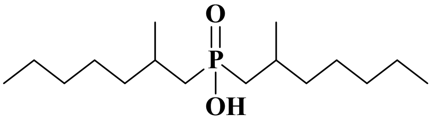

Bis(2-methylheptyl)phosphinic acid: ^{1}H NMR (400 MHz, CDCl3) δ 10.83 (s, 1H), 1.93 (s, 1H), 1.73-1.65 (m, 2H), 1.53-1.24 (m, 18H), 1.06-1.04 (dd, ^{1}J = 1.2Hz, ^{2}J = 1.2 Hz, 6H), 0.87 (t, J = 16 Hz, 6H). ^{13}C NMR(100 MHz, CDCl3) δ 38.82, 38.70, 37.61, 37.54, 36.71, 36.64, 31.94, 27.67, 26.40, 22.64, 21.27, 14.03. ^{31}P NMR (162 MHz, CDCl3) δ 60.12. ESI-MS(m/z): 289.25 (M-H$^+$). HRMS: calcd for $C_{16}H_{34}O_2P$ 289.2302; found 289.2295.

P227

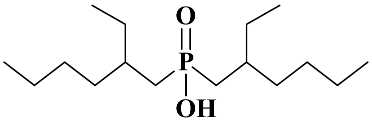

Bis(2-ethylhexyl)phosphinic acid: ^{1}H NMR (400 MHz, CDCl$_3$) δ 11.63 (s, 1H), 1.85 – 1.66 (m, 4H), 1.26 (bs, 18H), 1.12 (ddd, J = 16.7, 7.1, 2.0 Hz, 6H), 0.86 (t, J = 6.5 Hz, 6H). ^{31}P NMR (162 MHz, CDCl$_3$) δ 60.77. ESI-MS(m/z): 289.23 (M-H$^+$).